

# MOND orbits in the Solar System's periphery and confrontation with the observations

L. Iorio

*INFN-Sezione di Pisa. Address for correspondence: Viale Unità di Italia 68  
70125 Bari, Italy*

*tel./fax 0039 080 5443144*

*e-mail: lorenzo.iorio@libero.it*

## Abstract

We look for MONDian orbital effects in the outer regions of the Solar System by numerically integrating both the MOND (with  $\mu(X) = X/(1+X)$  which yields very good results with several type of galaxies) and the Newtonian equations of motions with the same initial conditions and investigate the resulting discrepancies from the classical picture. Major differences occur in the Oort cloud ( $r \approx 50 - 150$  kAU) where highly elongated orbits are not allowed by MOND, contrary to the Newtonian mechanics. This fact may have consequences on the composition and the dynamical history of the Oort cloud since the perturbations due to nearby passing stars, interstellar gas clouds and Galactic tides which in the classical framework change the velocities of the Oort's comets launching them in the inner regions of the Solar System would be less effective according to MOND. Then, we compare the predicted MOND effects for some trans-Neptunian objects (Pluto and Sedna,  $r \approx 40 - 500$  AU) and the giant gaseous planets Jupiter, Saturn, Uranus and Neptune ( $r \approx 5 - 30$  AU) with the optical observations gathered during the last century. The MOND effects for Sedna are orders of magnitude smaller than the present-day orbit accuracy, while those for Pluto over 100 yr are about of the same order of magnitude, or even larger, of its orbit accuracy which will be improved when the New Horizon spacecraft will encounter Pluto in 2015. The MONDian departures from the Newtonian paths over 80-100 yr for Neptune, Uranus, Saturn and Jupiter are, instead, quite larger than their orbit accuracy according to the latest DE (JPL, NASA), EPM (IAA, RAS) and INPOP (IMCCE) ephemerides in such a way that if MOND, not modelled in the dynamical force models of such ephemerides, was valid its effects should have been detected.

Keywords: gravitation-ephemerides-methods: numerical

# 1 Introduction

In many astrophysical systems like, e.g., spiral galaxies and clusters of galaxies a discrepancy between the observed kinematics of their exterior parts and the predicted one on the basis of the Newtonian dynamics and the matter detected from the emitted electromagnetic radiation (visible stars and gas clouds) was present since the pioneering studies by Bosma [1] and Rubin and coworkers [2] on spiral galaxies. More precisely, such an effect shows up in the galactic velocity rotation curves whose typical pattern after a few kpc from the center differs from the Keplerian  $1/\sqrt{r}$  fall-off expected from the usual dynamics applied to the electromagnetically-observed matter.

As a possible solution of this puzzle, the existence of non-baryonic, weakly-interacting Cold Dark (in the sense that its existence is indirectly inferred only from its gravitational action, not from emitted electromagnetic radiation) Matter (CDM) was proposed to reconcile the predictions with the observations [3] in the framework of the standard gravitational physics.

Oppositely, it was postulated that the Newtonian laws of gravitation have to be modified on certain acceleration scales to correctly account for the observed anomalous kinematics of such astrophysical systems without resorting to still undetected exotic forms of matter. One of the most phenomenologically successful modification of the inverse-square Newtonian law, mainly with respect to spiral galaxies, is the MODified Newtonian Dynamics (MOND) [4, 5, 6] which postulates that for systems experiencing total gravitational acceleration  $A < A_0$ , with [7]

$$A_0 = (1.2 \pm 0.27) \times 10^{-10} \text{ m s}^{-2}, \quad (1)$$

$$\mathbf{A} \rightarrow \mathbf{A}_{\text{MOND}} = -\frac{\sqrt{A_0 GM}}{r} \hat{\mathbf{r}}. \quad (2)$$

More precisely, it holds

$$A = \frac{A_N}{\mu(X)}, \quad X \equiv \frac{A}{A_0}; \quad (3)$$

$\mu(X) \rightarrow 1$  for  $x \gg 1$ , i.e. for large accelerations (with respect to  $A_0$ ), while  $\mu(X) \rightarrow x$  yielding eq. (2) for  $x \ll 1$ , i.e. for small accelerations. The most widely used forms for  $\mu$  are

$$\mu(X) = \frac{X}{1+X}, \quad [8] \quad (4)$$

$$\mu(X) = \frac{X}{\sqrt{1+X^2}} \quad [9]. \quad (5)$$

It recently turned out that the simpler form of eq. (4) yields much better results in fitting the terminal velocity curve of the Milky Way, the rotation curve of the standard external galaxy NGC 3198 [8, 10, 11] and of a sample of 17 high surface brightness, early-type disc galaxies [12]. Eq. (3) strictly holds for co-planar, spherically and axially symmetric mass distributions; otherwise, the full modified (non-relativistic) Poisson equation [9]

$$\nabla \cdot \left[ \mu \left( \frac{|\nabla U|}{A_0} \right) \nabla U \right] = 4\pi G\rho \quad (6)$$

must be used.

Attempts to yield a physical foundation to MOND, especially in terms of a relativistic covariant theory, can be found in, e.g., [13, 14, 15]; for recent reviews of various aspects of the MOND paradigm, see [16, 17, 18].

In this paper we will numerically integrate both the MOND and the Newtonian equations of motion in different acceleration regimes by using the same initial conditions in order to look for the departures  $\Delta r$  of the MONDian trajectories with respect to the Newtonian ones. After setting the theoretical background which we will use in the rest of the paper (Section 2), we will explore the strong MONDian regime in the remote ( $r = 50 - 150$  kAU) periphery of the Solar System, where the Oort cloud [19], populated by a huge number of small bodies moving along very eccentric and inclined to the ecliptic orbits, should exist (Section 3). In particular, we investigate the modifications that MOND would induce on the Newtonian orbits of a test particle moving in such a region; this will allow us to put forth some hypothesis on the overall configuration that the Oort cloud would have if MOND was valid. Then, we will move towards the inner regions of the Solar System populated by the trans-Neptunian objects (TNOs) where we will examine Sedna and Pluto (Section 4). Finally, we will look at the MONDian orbital effects on Neptune, Uranus, Saturn and Jupiter (Section 5). For other works mainly on MOND in Solar System, see Ref. [20, 21, 22, 23]. In particular, the authors of Ref. [20] and Ref. [23] dealt with the weak limits of the interpolating functions of eq. (4) and eq. (5) by examining the corrections  $\Delta\dot{\varpi}$  to the standard Newtonian/Einsteinian perihelion precessions of the inner planets recently estimated by E.V. Pitjeva in Ref. [24] with the EPM2004 ephemerides of the Institute of Applied Astronomy of the Russian Academy of Sciences. Since, at present, no other teams of astronomers have independently estimated their own anomalous perihelion precessions, in this paper we will follow a different approach by also using the ephemerides DE by the Jet Propulsion Laboratory (JPL) of NASA and INPOP by the Institut de Mécanique Céleste et de Calcul des Éphémérides (IMCCE). The

conclusions are in Section 6.

## 2 The MOND acceleration in the remote periphery of the Solar System

At heliocentric distances of 50-150 kAU the Newtonian acceleration due to the Sun is very weak amounting to only  $2 \times 10^{-12} - 10^{-13} \text{ m s}^{-2}$ , i.e. about  $0.02A_0$ ; thus, it is, in principle, an ideal scenario to look for strong MONDian effects. In the standard Newtonian framework, the Oort cloud is believed to be the reservoir of the long-period comets which are perturbed by nearby passing stars, Giant Molecular Clouds (GMCs) and Galactic tides [25] due to their highly elongated orbits. As a consequence of such interactions, temporary increases of the flux of comets entering the region of the planets-termed ‘‘comet showers’’-may occur [26, 27]. MOND may change such a picture.

In dealing with the MOND dynamics of an Oort-type object, the so-called External-Field-Effect (EFE) must also be taken into account, in principle, according to [16, 18]

$$\mu\left(\frac{A_{\text{ext}} + A}{A_0}\right)A = A_N, \quad (7)$$

where  $A_N$  is the Newtonian acceleration of the Sun-particle system alone,  $A$  is the total internal acceleration of the system, while  $A_{\text{ext}}$  denotes the acceleration induced by any field external to the system, not necessarily of tidal origin. By using the simpler form of eq. (4) for  $\mu$ , one obtains

$$A = \frac{A_N}{2} \left[ 1 - \frac{A_{\text{ext}}}{A_N} + \sqrt{\left(1 - \frac{A_{\text{ext}}}{A_N}\right)^2 + \frac{4A_0}{A_N} \left(1 + \frac{A_{\text{ext}}}{A_0}\right)} \right]. \quad (8)$$

For  $A_0 \rightarrow 0$ ,  $A \rightarrow A_N$ , as expected. For  $A_{\text{ext}} \rightarrow 0$ , i.e.  $A_{\text{ext}} \ll A_0$  and  $A_{\text{ext}} \ll A_N$ , one has

$$A \rightarrow \frac{A_N}{2} \left( 1 + \sqrt{1 + \frac{4A_0}{A_N}} \right). \quad (9)$$

For

$$\frac{A_{\text{ext}}}{A_0} \ll 1, \quad (10)$$

the total acceleration becomes

$$A \approx \frac{A_N}{2} \left[ 1 - \frac{A_{\text{ext}}}{A_N} + \sqrt{\left(1 - \frac{A_{\text{ext}}}{A_N}\right)^2 + \frac{4A_0}{A_N}} \right], \quad (11)$$

while for

$$\frac{A_{\text{ext}}}{A_N} \approx 1, \quad (12)$$

it is

$$A \approx \sqrt{A_N A_0 \left(1 + \frac{A_{\text{ext}}}{A_0}\right)}. \quad (13)$$

Interestingly, if

$$\frac{A_{\text{ext}}}{A_N} \approx 1, \quad \frac{A_{\text{ext}}}{A_0} \ll 1, \quad (14)$$

then

$$A \approx \sqrt{A_N A_0} = \frac{\sqrt{GM A_0}}{r}. \quad (15)$$

It must be stressed that, in MOND, effects like, e.g., the Galactic tides have not to be included in  $A_N$ , but in  $A_{\text{ext}}$ . Here we will neglect the stochastic interactions with other stars and interstellar clouds. The Galactic tidal acceleration is approximately given by

$$A_{\text{ext}} \approx \frac{GM_{\text{gal}} r}{R_{\odot}^3}, \quad (16)$$

where  $R_{\odot} = 8.5$  kpc is the Galactocentric distance of the Sun,  $M_{\text{gal}}$  is the mass of the Milky Way and  $r$  is the heliocentric distance of an Oort-like object. By assuming  $M_{\text{gal}} = 10^{11} M_{\odot}$ , it turns out

$$A_{\text{ext}} \approx 10^{-15} - 10^{-14} \text{ m s}^{-2}, \quad r = 50 - 150 \text{ kAU}. \quad (17)$$

Its effect on the Oort cloud have been worked out in the framework of the Newtonian dynamics by several authors; see, e.g., Ref. [28] and references therein. Thus, eq. (9) seems a reasonable approximation, as we will explicitly show. It is just the case of stressing that the centrifugal acceleration due to the Solar System's revolution around the Galactic center, which is of the order of  $A_{\text{cen}} = 10^{-10} \text{ m s}^{-2}$  since [29]  $v_{\odot} \approx 220 \text{ km s}^{-1}$ , does not play any role in the motion of the Solar System's bodies referred to the usual Solar System Barycenter (SSB) reference frame because  $A_{\text{cen}}$  is common to both SSB and the planets themselves which share their Galactic revolution with

the SSB. From a crude phenomenological point of view,  $A_{\text{cen}}$  would show up in the motion of all the planets as enormous anomalous secular perihelion precessions of more than 1 arcsec  $\text{cty}^{-1}$ , which are clearly ruled out by the latest determinations of the corrections to the standard apsidal precessions of the inner planets [24] accurate to the  $10^{-3} - 10^{-4}$  arcsec  $\text{cty}^{-1}$  level.

### 3 Numerically integrated MOND orbits in the Oort cloud

In order to see how MOND modifies the Newtonian dynamics of an Oort-type object, we perform two numerical integrations of the equations of motion in cartesian coordinates according to MOND and the Newtonian dynamics sharing the same initial conditions corresponding to the standard Keplerian ellipse. As a preliminary check of our assumptions concerning the possibility of neglecting EFE, we integrated the equations of motion with eq. (4) and eq. (8) by finding no differences. Thus, in the following we will use eq. (4). In Figure 1-Figure 3 we show how a Keplerian ellipse with inclination to the ecliptic  $i = 134$  deg, semimajor axis  $a = 87.46$  kAU and eccentricity  $e = 0.82$  would look like over a Keplerian orbital period  $P_b = 26$  Myr if MOND was valid. In Figure 4-Figure 5 we plot the distance and the speed as functions of time, while in Figure 6 we depict the speed as a function of the distance.

The orbit is still confined to a plane because of the conservation of the orbital angular momentum, but its shape and size are completely different. The minimum and, especially, the maximum heliocentric distances are quite smaller in MOND than in the Newtonian case; they are reached several times during one Keplerian orbital period (Figure 4). The speed attains almost always larger values in MOND than in Newtonian dynamics and it changes in time much frequently than in the Newtonian case (Figure 5). Moreover,  $v$  experiences a much more marked variation along the followed trajectory in MOND than in the Newtonian framework (Figure 6).

Such features may have consequences on the interaction of the Oort-like objects with passing stars [19] by reducing their perturbing effects and, thus, also altering the number of long-period comets launched into the inner regions of the Solar System, the number of comets left in the cloud throughout its history. Indeed, in the standard picture, the comets moving along very elongated orbits may come relatively close to a star of mass  $M_\star$  suffering a

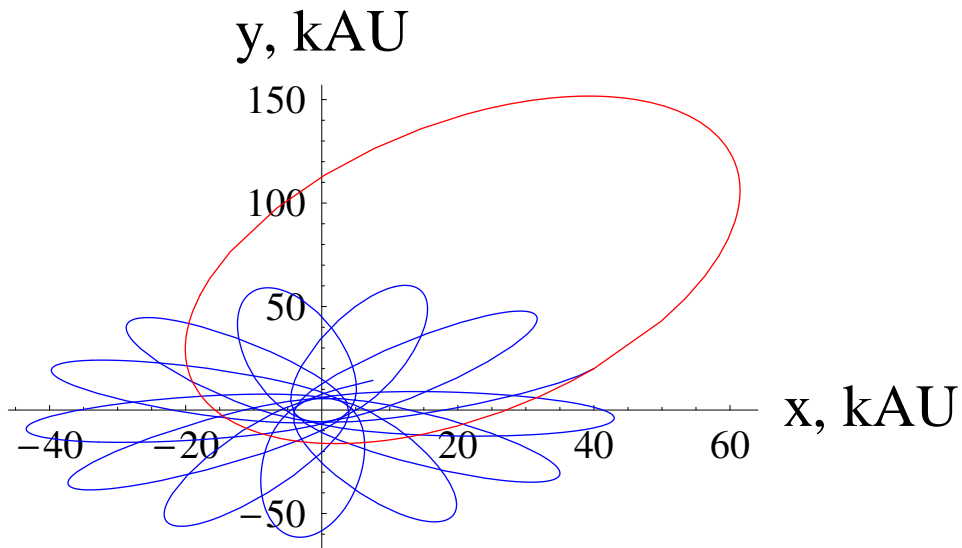


Figure 1: Sections in the  $\{x, y\}$  plane of the numerically integrated trajectories of two Oort-type test particles around the Sun, located at the origin, affected by the MONDian acceleration of eq. (4) (blue line) and the Newtonian monopole  $-GM/r^2$  (red line). For both particles it was assumed  $x_0 = 40$  kAU,  $y_0 = 20$  kAU,  $z_0 = 38$  kAU,  $\dot{x}_0 = -13$  kAU Myr $^{-1}$ ,  $\dot{y}_0 = -25$  kAU Myr $^{-1}$ ,  $\dot{z}_0 = -10$  kAU Myr $^{-1}$  (1 kAU Myr $^{-1} = 0.005$  km s $^{-1}$ ). They correspond to  $i = 134$  deg,  $a = 87.4$  kAU,  $e = 0.82$ . The integration interval correspond to the Keplerian orbital period  $P_b = 26$  Myr.

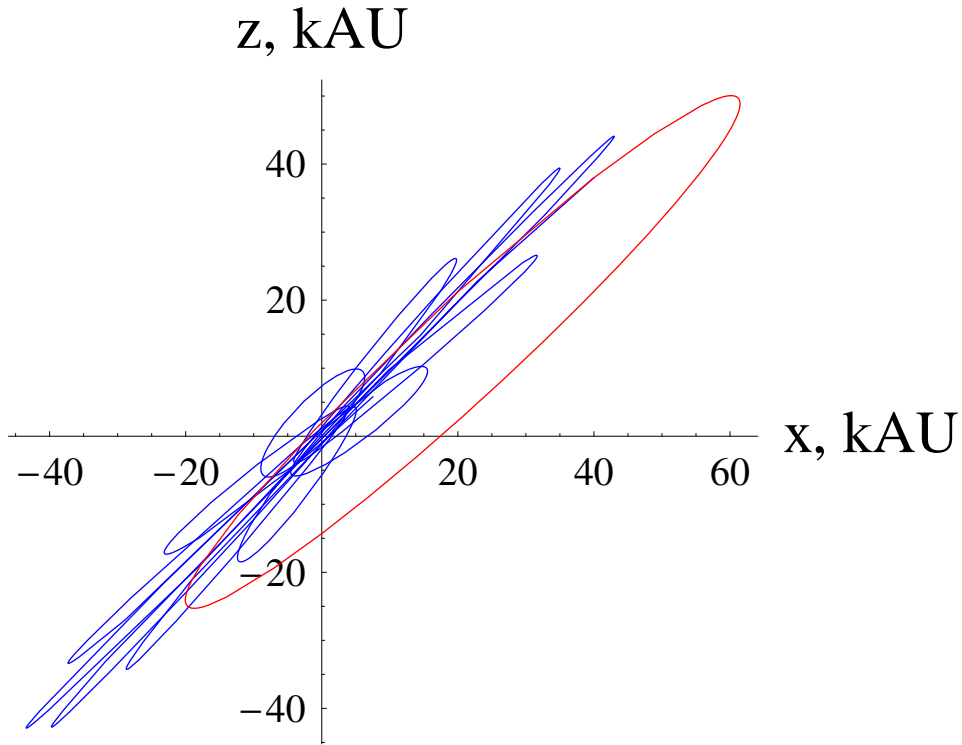


Figure 2: Sections in the  $\{x, z\}$  plane of the numerically integrated trajectories of two Oort-type test particles around the Sun, located at the origin, affected by the MONDian acceleration of eq. (4) (blue line) and the Newtonian monopole  $-GM/r^2$  (red line). For both particles it was assumed  $x_0 = 40$  kAU,  $y_0 = 20$  kAU,  $z_0 = 38$  kAU,  $\dot{x}_0 = -13$  kAU Myr $^{-1}$ ,  $\dot{y}_0 = -25$  kAU Myr $^{-1}$ ,  $\dot{z}_0 = -10$  kAU Myr $^{-1}$  (1 kAU Myr $^{-1} = 0.005$  km s $^{-1}$ ). They correspond to  $i = 134$  deg,  $a = 87.4$  kAU,  $e = 0.82$ . The integration interval correspond to the Keplerian orbital period  $P_b = 26$  Myr.

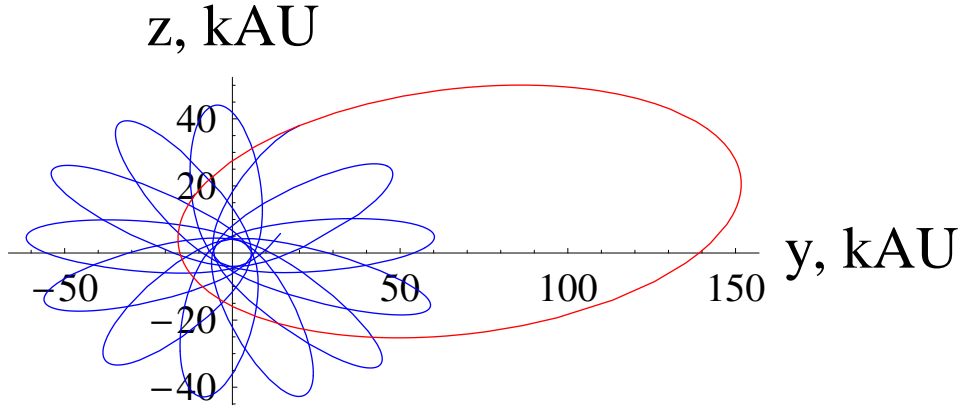


Figure 3: Sections in the  $\{y, z\}$  plane of the numerically integrated trajectories of two Oort-type test particles around the Sun, located at the origin, affected by the MONDian acceleration of eq. (4) (blue line) and the Newtonian monopole  $-GM/r^2$  (red line). For both particles it was assumed  $x_0 = 40$  kAU,  $y_0 = 20$  kAU,  $z_0 = 38$  kAU,  $\dot{x}_0 = -13$  kAU Myr $^{-1}$ ,  $\dot{y}_0 = -25$  kAU Myr $^{-1}$ ,  $\dot{z}_0 = -10$  kAU Myr $^{-1}$  (1 kAU Myr $^{-1} = 0.005$  km s $^{-1}$ ). They correspond to  $i = 134$  deg,  $a = 87.4$  kAU,  $e = 0.82$ . The integration interval correspond to the Keplerian orbital period  $P_b = 26$  Myr.

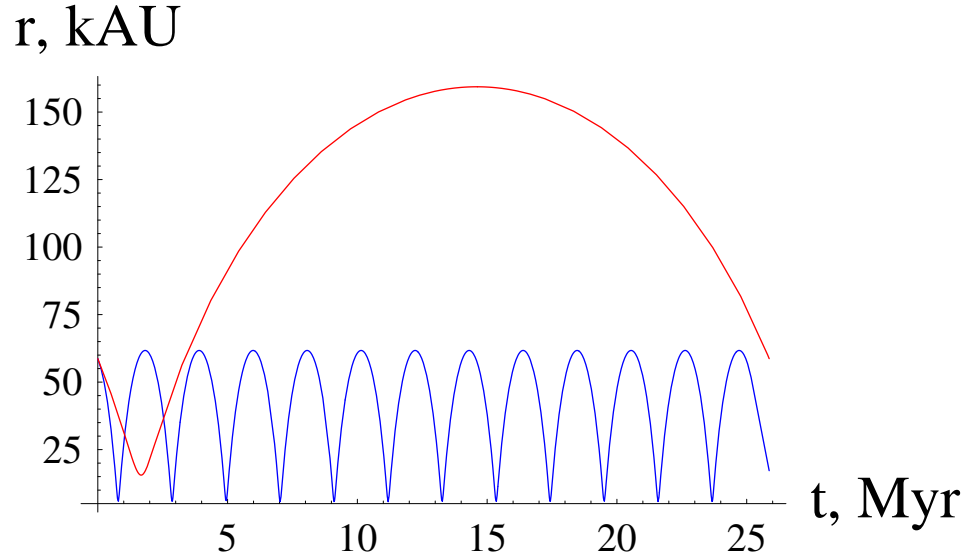


Figure 4: Blue line: heliocentric distance  $r$  (kAU) in MOND. Red line: heliocentric distance  $r$  (kAU) in Newtonian mechanics. The initial conditions are those of Figure 1-Figure 3. The time interval corresponds to the Keplerian orbital period  $P_b = 26$  Myr.

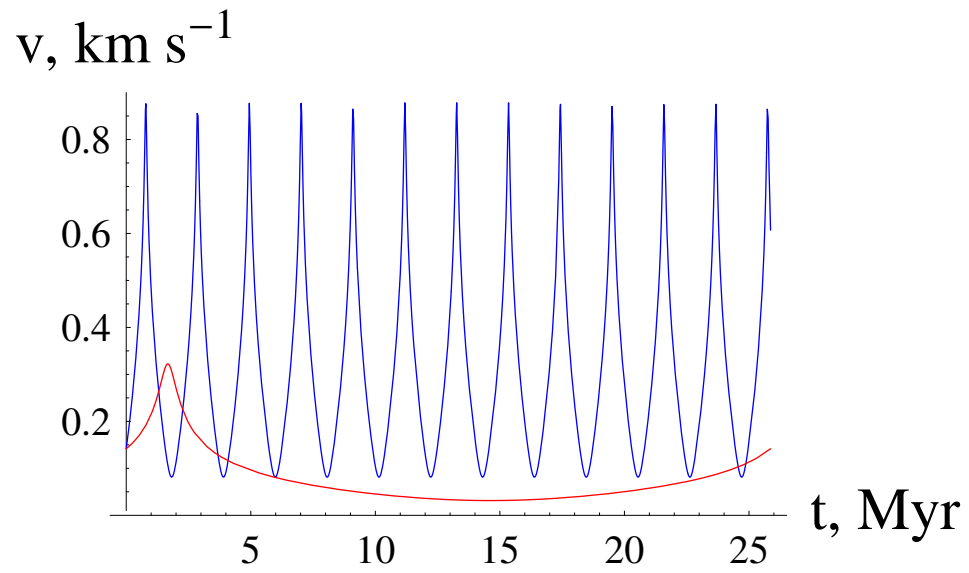


Figure 5: Blue line: speed  $v$  ( $\text{km s}^{-1}$ ) in MOND. Red line: speed  $v$  ( $\text{km s}^{-1}$ ) in Newtonian mechanics. The initial conditions are those of Figure 1-Figure 3. The time interval corresponds to the Keplerian orbital period  $P_b = 26$  Myr.

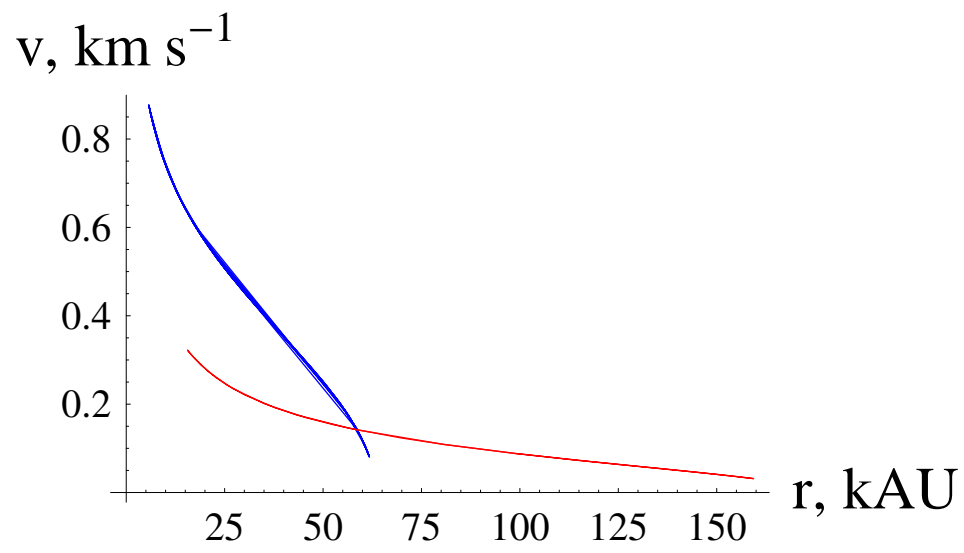


Figure 6: Blue line: speed  $v$  ( $\text{km s}^{-1}$ ) in MOND. Red line: speed  $v$  ( $\text{km s}^{-1}$ ) in Newtonian mechanics. The distance  $r$  is in kAU. The initial conditions are those of Figure 1-Figure 3.

change in velocity  $\Delta v$  which approximately is [19]

$$\Delta v = \frac{2GM_\star}{v_\star d}, \quad (18)$$

where  $v_\star$  is the star's velocity with respect to the Sun and  $d$  is the distance of closest approach with the Oort object. Moreover, less elongated orbits would also reduce the perturbing effects of the Galactic tides.

## 4 The trans-Neptunian objects

Let us, now examine the possibility of direct testing MOND by examining the orbital motions of some bodies in the closer periphery of the Solar System ( $r \gtrsim 0.03$  kAU). At first sight, such an idea may seem bizarre because MONDian departures from the usual Newtonian dynamics are expected to be negligible in such region where  $A_N/A_0 \approx 10^4$ , but, as we will see, they might be not excessively small with respect to the present-day level of accuracy in determining the orbital motions in the inner region of the TNOs field, at least for some selected bodies. In this Section we will straightforwardly use eq. (4) since the Galactic tidal effects are completely negligible with respect to both  $A_N$  and  $A_0$ . In Figure 7 we plot the difference between the heliocentric distances of 134340 Pluto ( $a = 39.5$  AU,  $e = 0.24$ ,  $i = 17.2$  deg), for which available observations since January 1914 exist, from two numerically integrated Newtonian and MONDian trajectories sharing the same initial conditions corresponding to 23 April 1965 retrieved from the HORIZONS system by NASA (<http://ssd.jpl.nasa.gov/?horizons>). MONDian deviations  $\Delta r$  from the Newtonian trajectory amount to about 20-200 Mm (1 Mm =  $10^6$  m) over 100 yr. Such values can be compared with the latest determinations of the Pluto's orbital elements. Since the average heliocentric distance is

$$\langle r \rangle = a \left( 1 + \frac{e^2}{2} \right), \quad (19)$$

its uncertainty can conservatively be evaluated as

$$\delta \langle r \rangle \leq \delta a \left( 1 + \frac{e^2}{2} \right) + ae\delta e. \quad (20)$$

According to Table 3 of [30], obtained with the EPM2006 ephemerides by E. V. Pitjeva, the formal, statistical uncertainty in  $a$  amounts to

$$\delta a = 34.1 \text{ Mm}, \quad (21)$$

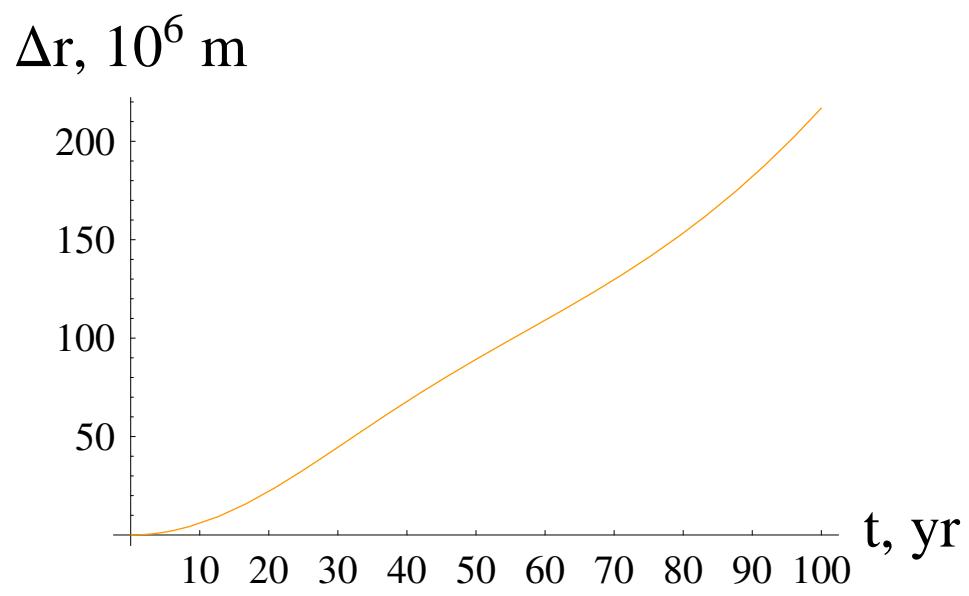


Figure 7: Difference  $\Delta r$  over 100 yr between the heliocentric distances of Pluto from two numerically integrated Newtonian and MONDian trajectories sharing the same initial conditions retrieved from the HORIZONS system by NASA.

while the uncertainty in the eccentricity  $e$  can be obtained from the non-singular elements  $h = e \cos \varpi$  and  $k = e \sin \varpi$  as

$$\delta e \leq \frac{|h|\delta h + |k|\delta k}{e} = 2 \times 10^{-6}. \quad (22)$$

Thus, the uncertainty in the average heliocentric distance of Pluto is

$$\delta \langle r \rangle_{\text{Pluto}} \lesssim 59.5 \text{ Mm}. \quad (23)$$

The result of eq. (23) tells us that the predicted MONDian departures from the Newtonian orbit of Pluto after about 30 yr would be measurable; thus, it might be argued that, since no deviations from the usual Newtonian behavior as large as those predicted by MOND have been so far detected in the Pluto's data, MOND would be in trouble. However, caution is in order because it must be noted that eq. (23) has been obtained by taking the  $1 - \sigma$  formal uncertainties; since only relatively inaccurate optical data are available so far for Pluto, the realistic error in its orbit may be, very conservatively, up to 10 times larger. On the other hand, according to Fig. 14 by Folkner et al. [31], the uncertainty in the Pluto heliocentric distance, evaluated as the difference between the DE418 and DE414 ephemerides from 1900 to 2020, may be up to 20 Mm. Smaller figures, of the order of 1 – 5 Mm, are quoted in Figure 15 and Figure 16 of Ref. [31] in which the interval 1920-2020 is considered. The difference between the DE405 and INPOP06 ephemerides over 100 yr quoted in Table 4, 2nd column, of Ref. [32] yields an uncertainty in the heliocentric range of Pluto of 35 Mm. By the way, the situation may change in the near future because Pluto is the target of the spacecraft-based New Horizons mission which should greatly improve, among other things, also our knowledge of the orbit of Pluto, to be reached in 2015.

It maybe interesting to look also at 90377 Sedna (2003 VB12) ( $a = 514$  AU,  $e = 0.85$ ,  $i = 11.9$  deg), for which available observations since September 1990 exist, to have an idea of what could be the perspectives in using it for testing MOND; after all, the MONDian effects on Sedna should be larger than on Pluto. By proceeding as for Pluto, we see in Figure 8 that the MONDian departures  $\Delta r$  from the Newtonian trajectory amount to about 0.0005 – 0.003 AU over 100 yr, while

$$\delta \langle r \rangle_{\text{Sedna}} \lesssim 3.3 \text{ AU}, \quad (24)$$

where we used the formal  $1 - \sigma$  uncertainties  $\delta a = 2.2203$  AU,  $\delta e = 0.00070246$  retrieved from the JPL Small-Body Database Browser (<http://ssd.jpl.nasa.gov/sbdb.cgi>).

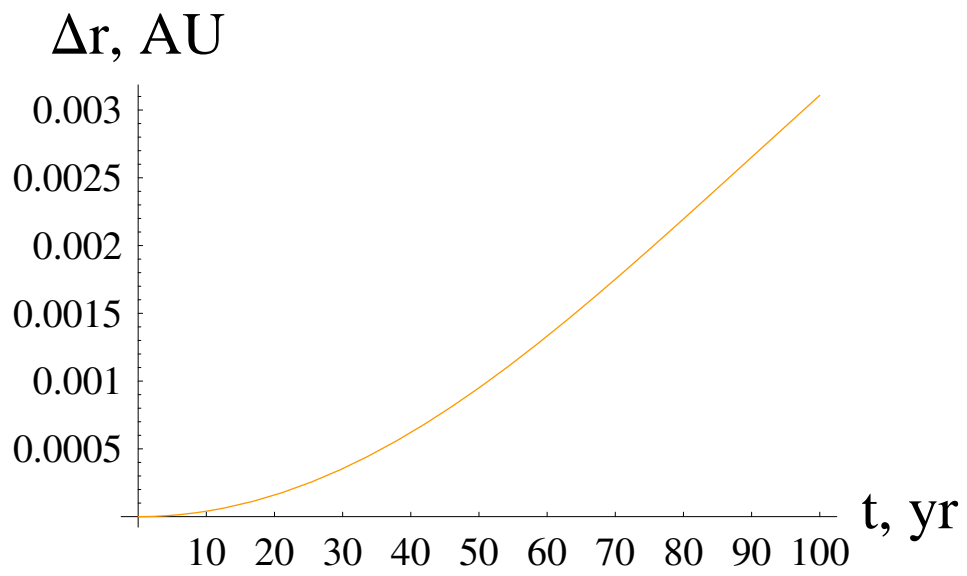


Figure 8: Difference  $\Delta r$  over 100 yr between the heliocentric distances of Sedna from two numerically integrated Newtonian and MONDian trajectories sharing the same initial conditions retrieved from the HORIZONS system by NASA.

In this case, the MOND-induced shift of Sedna is 3 – 4 orders of magnitude smaller than the present-day accuracy in knowing its orbit.

Summarizing this Section, Sedna is the body which, in principle, exhibits the largest MONDian orbital effects among the trans-Neptunian objects, but the present-day accuracy in knowing its orbit is too poor by 3 – 4 orders of magnitude to appreciate them. The case of Pluto is more interesting because the MONDian effects on its path are about of the same order of magnitude, or even larger, of its orbital accuracy which should be improved in the mid future thanks to the New Horizon mission. By the way, the present-day situation for Pluto does not allow to infer a firm conclusion about its MONDian effects.

## 5 The giant gaseous planets

Leaving the TNOs to move towards the region of the giant gaseous planets, it turns out that the MOND trajectory of Neptune ( $a = 30$  AU,  $e = 0.008$ ,  $i = 1.8$  deg) deviates from the Newtonian one by  $\Delta r \approx 20 - 150$  Mm over 100 yr, as depicted by Figure 9. Quite interestingly, the numerous optical observations for Neptune processed by Pitjeva [30] yield

$$\delta \langle r \rangle_{\text{Neptune}} \leq 0.8 \text{ Mm}, \quad (25)$$

where we used the formal  $1 - \sigma$  uncertainties [30]  $\delta a = 0.46$  Mm,  $\delta e = 0.0000105326$ . In this case, even by re-scaling them by a factor 10, the MOND effect should have not escaped from detection if it existed. Another way to deal with the problem of assessing the realistic accuracy in knowing Neptune’s orbit from optical data is as follows. The latest Charge Coupled Device (CCD)-based observations of the outer planets are accurate to about [30] 0.06 arcsec level; this translates into an about 1 – 1.6 Mm accuracy at Neptune’s distance which becomes about 4 Mm if one considers the  $\approx 0.2$  arcsec accuracy of the older photographic observations. The confrontation between the DE410 and DE405 ephemerides from 1970 to 2010 in Fig. 2 of Ref. [33] yields an uncertainty up to about 1 Mm. Table 4, 2nd column, in Ref. [32] yields 3.2 Mm for the uncertainty in the Neptune’s heliocentric distance over 100 yr evaluated as difference between the DE405 and INPOP06 ephemerides. Thus, MOND seems seriously challenged by Neptune.

The situation for Uranus ( $a = 19$  AU,  $e = 0.046$ ,  $i = 0.77$  deg), whose MOND discrepancy from the Newtonian case over 100 yr is shown in Figure 10, is even more neat. Indeed, its maximum value is of the order of 40 Mm, while Table 3 of Ref. [30] yield for the formal  $1 - \sigma$  errors  $\delta a = 0.04$  Mm

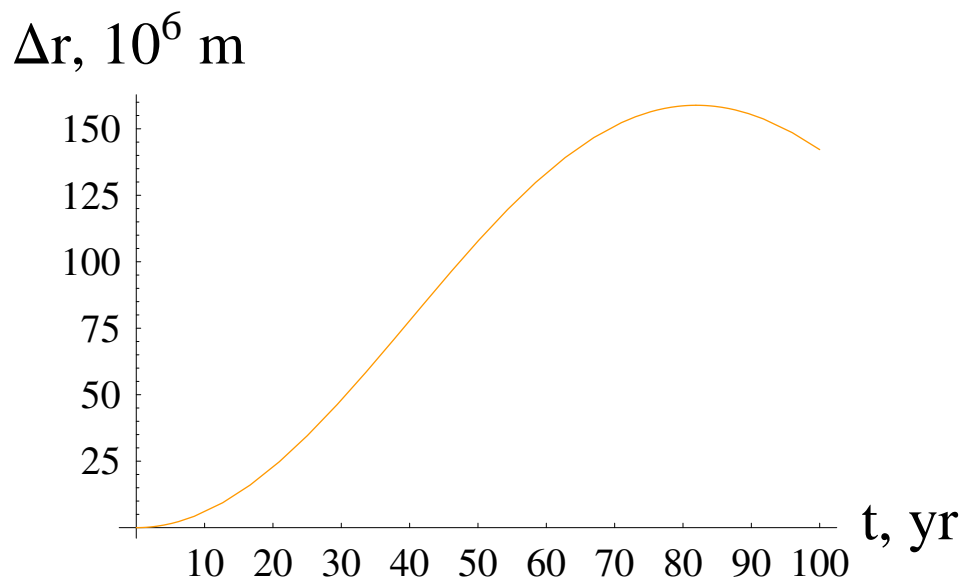


Figure 9: Difference  $\Delta r$  over 100 yr between the heliocentric distances of Neptune from two numerically integrated Newtonian and MONDian trajectories sharing the same initial conditions retrieved from the HORIZONS system by NASA.

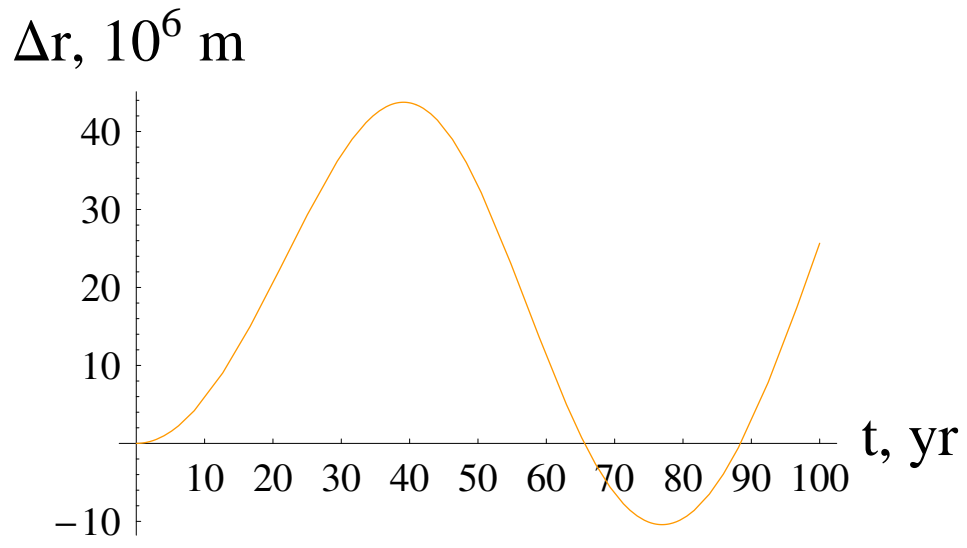


Figure 10: Difference  $\Delta r$  over 100 yr between the heliocentric distances of Uranus from two numerically integrated Newtonian and MONDian trajectories sharing the same initial conditions retrieved from the HORIZONS system by NASA.

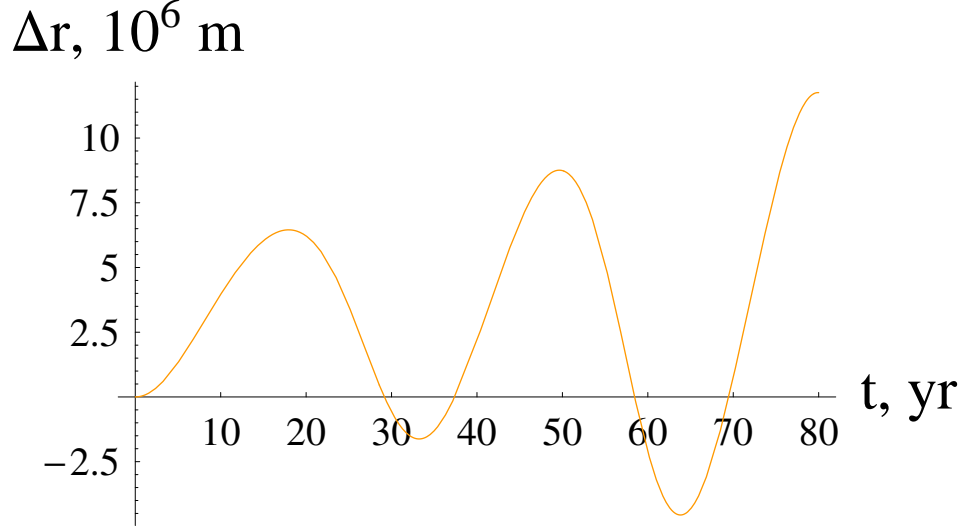


Figure 11: Difference  $\Delta r$  over 80 yr between the heliocentric distances of Saturn from two numerically integrated Newtonian and MONDian trajectories sharing the same initial conditions retrieved from the HORIZONS system by NASA.

and  $\delta e = 4 \times 10^{-7}$ , so that

$$\delta \langle r \rangle_{\text{Uranus}} \leq 0.1 \text{ Mm}. \quad (26)$$

By re-scaling it by a factor 10 or, equivalently, by mapping the angular error of 0.1 arcsec into a radial uncertainty at the Uranus' distance, one gets about 1 Mm. The same result is also obtained in Figure 2 of Ref. [33] by comparing the DE410 and DE405 ephemerides from 1970 to 2010, and in 2nd column of Table 4 in Ref. [32] by taking the difference over 100 yr between the DE405 and INPOP06 ephemerides. Such a level of accuracy is good enough to have allowed for the detection of the MOND effects on Uranus.

The MONDian behavior of Saturn ( $a = 9.5 \text{ AU}$ ,  $e = 0.055$ ,  $i = 2.5 \text{ deg}$ ) with respect to the Newtonian one over 80 yr is depicted in Figure 11. The discrepancy lies in the range 1 – 10 Mm, while Table 3 of Ref. [30], in which only optical data have been used, yields the formal  $1 - \sigma$  errors  $\delta a = 4256 \text{ m}$ ,  $\delta e = 4 \times 10^{-7}$ , so that

$$\delta \langle r \rangle_{\text{Saturn}} \leq 0.04 \text{ Mm}. \quad (27)$$

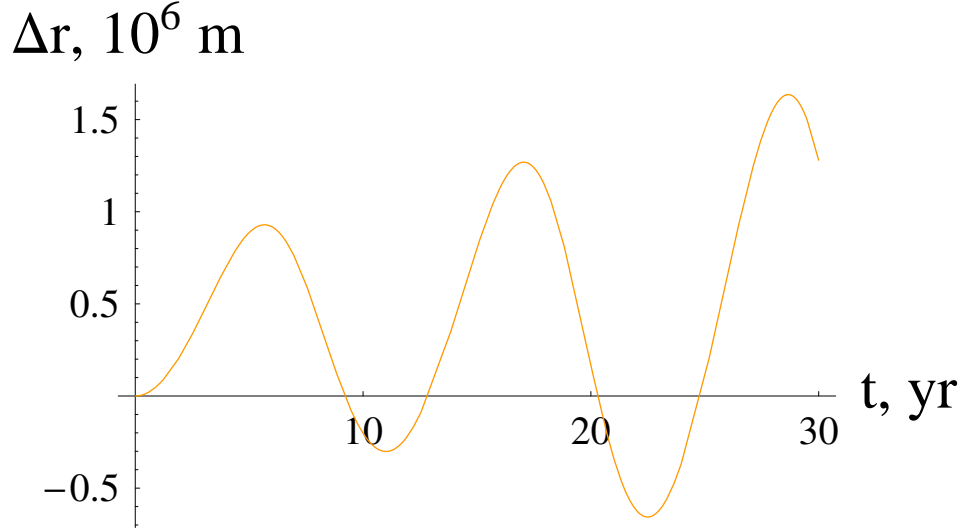


Figure 12: Difference  $\Delta r$  over 80 yr between the heliocentric distances of Jupiter from two numerically integrated Newtonian and MONDian trajectories sharing the same initial conditions retrieved from the HORIZONS system by NASA.

Figure 2 of Ref. [33], obtained by comparing the DE410 and DE405 ephemerides from 1970 to 2010, yields a maximum uncertainty of 0.2 Mm. Table 4, 2nd column of Ref. [32] yields an uncertainty of 0.29 Mm in the heliocentric distance of Saturn by taking the difference between the DE405 and INPOP06 ephemerides over 100 yr.

The case of Jupiter ( $a = 5.2 \text{ AU}$ ,  $e = 0.048$ ,  $i = 1.3 \text{ deg}$ ), for which also radiometric observations from several spacecrafts (Pioneer 10-11, Voyager, Ulysses, Galileo) have been used in, e.g., [30], is shown in Figure 12. The MOND effect lies in the range 0.1-1.5 Mm over 30 yr, while the formal  $1 - \sigma$  errors in  $a$  and  $e$  in Table 3 of [30] yield

$$\delta \langle r \rangle_{\text{Jupiter}} \leq 0.002 \text{ Mm}. \quad (28)$$

Fig. 2 of Ref. [33] shows the difference between the DE410 and DE405 ephemerides from 1970 to 2010; the maximum uncertainty in  $r$  is about 0.02 Mm. The uncertainty in  $r$ , evaluated as difference between the DE405 and INPOP06 ephemerides over 100 yr, quoted in Table 4, 2nd column of [32] amounts to 0.03 Mm.

In principle, one should also include the mutual  $N$ -body interactions

between all the major bodies of the Solar System in  $A_N$  when both the MONDian and the Newtonian equations of motion are integrated, but it is unlikely that they can substantially alter the results obtained so far.

It might be argued that, since MOND was not modelled in the ephemerides considered, the fact that its predicted effects do not show up in the observed planetary motions may be due to some sort of total/partial “absorption” of the MONDian effects in the estimation of the planets’ initial state vectors; as a consequence, one should explicitly model MOND and estimate, among other things, a dedicated parameter explicitly accounting for it. On the other hand, it could be argued that the size of the predicted MOND effects is so large that such a simultaneous removal of its signature from all the planets’ determined orbits seems unlikely.

In summary, the accuracy in our knowledge of the orbits of Neptune, Uranus, Saturn and Jupiter is good enough to having allowed for a detection of the relatively large MOND effects, for  $\mu(X) = X/(1 + X)$ , on their trajectories.

## 6 Summary and conclusions

We have numerically investigated the orbital motions of test particles according to MOND in different regions of the Solar System: the Oort cloud ( $r \approx 50 - 150$  kAU), the mid-inner Kuiper belt ( $r \approx 40 - 500$  AU) and the outer region of the gaseous giant planets ( $r \approx 5 - 30$  AU). As MONDian interpolating function  $\mu(X)$ , we used the form  $\mu(X) = X/(1 + X)$  which recently turned out to yield much better results in the galaxies realm than the older one  $\mu = X/\sqrt{1 + X^2}$ . We integrated both the MOND and the Newtonian equations of motion in Cartesian coordinates sharing the same initial conditions retrieved with the HORIZONS software by NASA and compared the resulting orbital trajectories; for Jupiter, Saturn, Uranus, Neptune, Pluto and Sedna we also computed the difference  $\Delta r$  between the resulting heliocentric distances over 100 yr.

The structure and the dynamical history of the Oort cloud, in deep MONDian regime, would be altered with respect to the standard Newtonian picture because highly eccentric orbits would not be allowed by MOND which, on the contrary, strongly tends to shrink them. As a consequence, one may speculate that the number of long-period comets launched in the inner parts of the Solar System should be reduced because of the less effective perturbing actions of nearby passing stars, interstellar clouds and Galactic tides.

In the Kuiper belt, Sedna exhibits MOND departures from the standard Newtonian picture which are orders of magnitude smaller than the present-day accuracy in determining its orbit. The situation for Pluto is more favorable because the MOND effects on it over one century are about of the same order of magnitude, or even larger, of its orbital accuracy. Moreover, it should be improved by the ongoing New Horizons mission which should reach Pluto in 2015.

Concerning Neptune, Uranus, Saturn and Jupiter their MONDian departures from the Newtonian paths over a time span of 80-100 yr, computed by neglecting in  $A_N$  the  $N$ -body mutual interactions with the other major bodies of the Solar System, are, in fact, 1 order of magnitude, or even more, larger than the realistic accuracy in determining their orbits from modern optical observations processed with various ephemerides produced by different institutions (EPM by Institute of Applied Astronomy of the Russian Academy of Sciences, DE by Jet Propulsion Laboratory of NASA, INPOP by Institut de Mécanique Céleste et de Calcul des Éphémérides) over just one century. Since such effects have not been detected so far, this poses a serious challenge to the validity of MOND, with the interpolating function used here, in the Solar System, in agreement with the results obtained in previous studies by using the corrections  $\Delta\dot{\omega}$  to the standard Newtonian/Einsteinian perihelion precessions estimated by E.V. Pitjeva with the EPM ephemerides. In principle, there is the possibility that the MONDian signatures, not modelled in the ephemerides used to process the data, may have been totally/partially removed in the estimation process of the planetary initial conditions; on the other hand, it may be noted that the size of the MOND effects is so large that it is unlikely that such a uniform removal from all the planets' determined orbits may have occurred. Anyway, a complementary test that could be done may consist in explicitly modeling MOND in the dynamical force models of the ephemerides and estimating, among other things, an ad-hoc, dedicated parameter accounting for it.

## Acknowledgments

I thank P. Salucci for having strongly encouraged me to rewrite the paper focussing on the Solar System.

## References

- [1] A. Bosma, “21-cm line studies of spiral galaxies. I - Observations of the galaxies NGC 5033, 3198, 5055, 2841, and 7331. II - The distribution and kinematics of neutral hydrogen in spiral galaxies of various morphological types”, *The Astronomical Journal*, vol. 86, December 1981, pp. 1791-1846, 1981.
- [2] V. C. Rubin, W. K. Ford, N. Thonnard, and D. Burstein, “Rotational properties of 23 SB galaxies”, *The Astrophysical Journal*, vol. 261, October 15, pp. 439-456, 1982.
- [3] V. C. Rubin, “The Rotation of Spiral Galaxies”, *Science*, vol. 220, no. 4604, pp. 1339-1344, 1983.
- [4] M. Milgrom, “A Modification of the Newtonian Dynamics as a Possible Alternative to the Hidden Mass Hypothesis”, *The Astrophysical Journal*, vol. 270, July 15, pp. 365-370, 1983a.
- [5] M. Milgrom, “A Modification of the Newtonian Dynamics - Implications for Galaxies”, *The Astrophysical Journal*, vol. 270, July 15, pp. 371-389, 1983b.
- [6] M. Milgrom, “A Modification of the Newtonian Dynamics - Implications for Galaxy Systems”, *The Astrophysical Journal*, vol. 270, July 15, pp. 384-389, 1983c.
- [7] K. G. Begeman, A. H. Broeils, and R. H. Sanders, “Extended rotation curves of spiral galaxies - Dark haloes and modified dynamics”, *Monthly Notices of the Royal Astronomical Society*, vol. 249, April 1, pp. 523-537, 1991.
- [8] B. Famaey, and J. Binney, “Modified Newtonian dynamics in the Milky Way”, *Monthly Notices of the Royal Astronomical Society*, vol. 363, no. 2, pp. 603-608, 2005.
- [9] J. D. Bekenstein, and M. Milgrom, “Does the Missing Mass Problem Signal the Breakdown of Newtonian Gravity?”, *The Astrophysical Journal*, vol. 286, November 1, pp. 7-14, 1984.
- [10] H. Zhao, and B. Famaey, “Refining the MOND Interpolating Function and TeVeS Lagrangian”, *The Astrophysical Journal*, vol. 638, no. 1, pp. L9-L12, 2006.

- [11] B. Famaey, G. Gentile, J.-P. Bruneton, and H. Zhao, “Insight into the baryon-gravity relation in galaxies”, *Physical Review D*, vol. 75, no. 6, 063002, 2007.
- [12] R. H. Sanders, and E. Noordermeer, “Confrontation of MODified Newtonian Dynamics with the rotation curves of early-type disc galaxies”, *Monthly Notices of the Royal Astronomical Society*, vol. 379, no. 2, pp. 702-710, 2007.
- [13] J. D. Bekenstein, “Relativistic gravitation theory for the modified Newtonian dynamics paradigm”, *Physical Review D*, vol. 70, no. 8, id. 083509, 2004.
- [14] J.-P. Bruneton, and G. Esposito-Farèse, “Field-theoretical formulations of MOND-like gravity”, *Physical Review D*, vol. 76, no. 12, id. 124012, 2007.
- [15] H. Zhao, “Coincidences of Dark Energy with Dark Matter: Clues for a Simple Alternative?”, *The Astrophysical Journal*, vol. 671, no. 1, pp. L1-L4, 2007.
- [16] R. H. Sanders, and S. S. McGaugh, “Modified Newtonian Dynamics as an Alternative to Dark Matter”, *Annual Review of Astronomy and Astrophysics*, vol. 40, September 2002, pp. 263-317, 2002.
- [17] J. D. Bekenstein, “The modified Newtonian dynamics - MOND and its implications for new physics”, *Contemporary Physics*, vol. 47, no. 6, pp. 387-403, 2006.
- [18] M. Milgrom, “The MOND paradigm”, Talk presented at the XIX Rencontres de Blois “Matter and energy in the Universe: from nucleosynthesis to cosmology”, May 2007, <http://arxiv.org/abs/0801.3133v2>.
- [19] J. H. Oort, “The structure of the cloud of comets surrounding the Solar System and a hypothesis concerning its origin”, *Bullettin of the Astronomical Institutes of The Netherlands*, vol. 11, no. 408, pp. 91-110, 1950.
- [20] M. Sereno, and Ph. Jetzer, “Dark matter versus modifications of the gravitational inverse-square law: results from planetary motion in the Solar system”, *Monthly Notices of the Royal Astronomical Society*, vol. 371, no. 2, pp. 626-632, 2006.

- [21] J. D. Bekenstein, and J. Magueijo, “Modified Newtonian dynamics habitats within the solar system”, *Physical Review D*, vol. 73, no. 10, id. 103513, 2006.
- [22] R. H. Sanders, “Solar system constraints on multifield theories of modified dynamics”, *Monthly Notices of the Royal Astronomical Society*, vol. 370, no. 3, pp. 1519-1528, 2006.
- [23] L. Iorio, “Constraining MOND with Solar System dynamics”, *Journal of Gravitational Physics*, vol. 2, no. 1, pp. 26-32, 2008.
- [24] E. V. Pitjeva, “Relativistic Effects and Solar Oblateness from Radar Observations of Planets and Spacecraft”, *Astronomy Letters*, vol. 31, no. 5, pp. 340-349, 2005.
- [25] A. Moribidelli, “Origin and Dynamical Evolution of Comets and their Reservoirs”, <http://arxiv.org/abs/astro-ph/0512256>, 2005.
- [26] J., Heisler, S. Tremaine, and C. Alcock, “The frequency and intensity of comet showers from the Oort cloud”, *Icarus*, vol. 70, no. 2, pp. 269-288, 1987.
- [27] J. J. Matese, P. G. Whitman, K. A. Innanen, and M. J. Valtonen, “Periodic Modulation of the Oort Cloud Comet Flux by the Adiabatically Changing Galactic Tide”, *Icarus*, vol. 116, no. 2, pp. 255-268, 1995.
- [28] M. Fouchard, C. Froeschlé, G. Valsecchi, and H. Rickman, “Long-term effects of the Galactic tide on cometary dynamics”, *Celestial Mechanics and Dynamical Astronomy*, vol. 95, no. 1-4, pp. 299-326, 2006.
- [29] B. Famaey, *Kynematics and Dynamics of Giant Stars in the Solar Neighbourhood*, *PhD Thesis*, Universite Libre de Bruxelles, Faculté des Sciences, 2003.
- [30] E. V. Pitjeva, “Use of optical and radio astrometric observations of planets, satellites and spacecraft for ephemeris astronomy” in: W. J. Jin, I. Platais, and M. A. C. Perryman (eds.), *A Giant Step: from Milli- to Micro-arcsecond Astrometry, Proceedings of the International Astronomical Union, IAU Symposium, Volume 248*, pp. 20-22, 2008.
- [31] W. M. Folkner, E. M. Standish, J. G. Williams, and D. H. Boggs. “Planetary and lunar ephemeris DE418”, *Interoffice Memorandum IOM 343R-07-005*, 2008. (<ftp://ssd.jpl.nasa.gov/pub/eph/planets/ioms/>)

- [32] A. Fienga, H. Manche, J. Laskar, and M. Gastineau, “INPOP06: a new numerical planetary ephemeris”, *Astronomy and Astrophysics*, vol. 477, no. 1, pp. 315327, 2008.
- [33] E. M. Standish jr., “JPL Planetary and Lunar Ephemerides, DE414”, *Interoffice Memorandum IOM 343R-06-002*, 2006.